

Fluid Flow in Composite Regions Past a Solid Sphere

Umadevi Ramanna¹ , Chadrashekhhar Dasarahalli Venkataiah² ,

Dinesh Pobbathy Ashwathnarayana^{3,*} , Jayalakshamma Dasarahalli Venkataiah⁴ ,

Makam Swaminathan⁵ 

¹ Department of Basic Sciences, Atria Institute of Technology (Affiliated to VTU), Bangalore -560024, Karnataka, India; umadevi.r@atria.edu (U.R);

² Department of Basic Sciences & Humanities, Vivekananda Institute of Technology, Bengaluru – 560 074, Karnataka, India; dvchandru@gmail.com (D.V.C);

³ Department of Mathematics, M S Ramaiah Institute of Technology, Bengaluru – 560 054, Karnataka, India; dineshdpa@msrit.edu (D.P.A);

⁴ Department of Mathematics, Vemana Institute of Technology, Bengaluru - 560034, Karnataka, India; jaya.dvj@gmail.com (D.V.J.);

⁵ Department of Mathematics, B M S College of Engineering, Bengaluru – 560 019, Karnataka, India; msgayathri.maths@bmsce.ac.in (M.S.G);

* Correspondence: dineshdpa@msrit.edu;

Scopus Author ID 55934627800

Received: 2.08.2021; Revised: 20.09.2021; Accepted: 25.09.2021; Published: 16.10.2021

Abstract: A steady, 2-D, incompressible, viscous fluid flow past a stationary solid sphere of radius 'a' has been considered. The flow of fluid occurs in 3 regions, namely fluid, porous and fluid regions. The governing equations for fluid flow in the clear and porous regions are Stokes and Brinkman equations, respectively. These governing equations are written in terms of stream function in the spherical coordinate system and solved using the similarity transformation method. The variation in flow patterns by means of streamlines has been analyzed for the obtained exact solution. The nature of the streamlines and the corresponding tangential and normal velocity profiles are observed graphically for the different values of porous parameter ' σ '. From the obtained results, it is noticed that an increase in porous parameters suppresses the fluid flow in the porous region due to less permeability; as a result, the fluid moves away from the solid sphere. It also decreases the velocity of the fluid in the porous region due to the suppression of the fluid as ' σ ' increases. Hence the parabolic velocity profile is noticed near the solid sphere.

Keywords: fluid flow, Brinkman equation; Stokes equation; interface boundary; permeability parameter.

© 2021 by the authors. This article is an open-access article distributed under the terms and conditions of the Creative Commons Attribution (CC BY) license (<https://creativecommons.org/licenses/by/4.0/>).

1. Introduction

The fluid flow through the porous medium is of considerable interest as it is important in natural occurrence. It has great significance in the fields of industrial, geophysical, and biomedical uses. The porous medium is used in chemical industries to obtain a powerful mixing process, filtration, purification, and oil recovery. In nuclear industries, it has been used for effective insulation and emergency cooling of nuclear reactors. In the bio-medical field, to understand the transport process of lungs and kidneys, the flow of fluid through porous media is essential.

In the literature, there are numerous models to illustrate the flow of fluid through the porous media. One such model had been established by Ooms *et al.* [1], which is valid for non-homogeneous porous medium. In the view of flow behavior and porousness of the medium, the extensively applicable model is preferably the Brinkman model. Saffman *et al.* [2] and Neale *et al.* [3] stated the advantages of the Brinkman model over the Darcy model, and Howells *et al.* [4] gave the theoretical explanations for the validity of the Brinkman equation. The problem of porous bodies before the Stokes flow for the mixed zone has been studied by Masliyah *et al.* [5], Qin and Kaloni *et al.* [6], Pop and Ingham *et al.* [7], and Anindita Bhattacharya *et al.* [8]. They have used the Brinkman model in the porous region to describe the motion of the fluid by considering uniform velocity away from the sphere.

A fully developed electrically conducting fluid flow in a fluid-saturated porous medium channel with the influence of parallel Lorentz force was investigated by Pantokratoras *et al.* [9]. They found that because of less conductivity of the fluid and also due to certain adjustments of magnetic and electric fields made in the lower plate, Lorentz force fluctuates in the vertical direction. The effect of steady non-uniform fluid flow through porous media on the velocity of the fluid, in which the porous media consisting of different pores having different angles of inclination, was studied by Bhanu Prakasham Reddy *et al.* [10]. They observed that, as a result of an increase in the angle of inclination, the velocity of the considered fluid flow also increases. The micropolar fluid flow past an impermeable sphere was studied numerically by Jayalakshamma *et al.* [11], assuming that the uniform fluid flow far away from the sphere. It was noticed that the viscous sublayer reduces, and velocity magnifies with an increase in coupling number. Mahabaleshwar *et al.* [12] considered the flow of fluid through a semi-infinite porous media with one boundary subject to the slipping of the fluid, the solid being proportionally sheared, and the fluid being injected at the boundary. They obtained the analytical solution by a similarity transformation method and determined the effects of the boundary conditions on the flow through the porous media. Siva *et al.* [13] investigated the effect of pressure drop on the parameters like a bed to particle diameter ratio, the shape of the porous material, porosity and established the direct empirical correlations for the same. Satya *et al.* [14] studied incompressible, viscous fluid flow through a porous cylinder embedded in another infinite porous medium. They investigated a new result for the drag force experienced by the porous cylinder. Also, the dependence of the drag coefficient, shear stress, streamlines patterns, and velocity profiles for various values of parameters are presented graphically. Further micropolar fluid flow past a sphere enclosing a solid core that is embedded in a porous medium was explored by Krishnan Ramalakshmi *et al.* [15]. They analyzed the drag coefficient and its dependence with a variation of permeability parameter numerically and discussed it graphically. Khanukaevaa *et al.* [16] studied the effect of permeability parameter, particle volume fraction, micro polarity number, etc., on hydrodynamic permeability of membrane by considering the micropolar fluid flow through a membrane presented as a swarm of dense cylindrical particles with porous layer. It was found that hydrodynamic permeability is very dependent on the perviousness of the membrane.

Umadevi *et al.* [17] developed a mathematical model to study the synchronized effects of particle drag and slip parameters on velocity and flow rate in an annular cross-sectional region bounded by two eccentric cylinders. A theoretical analysis was carried out by Sravan Kumar *et al.* [18] to draw out the flow characteristics of natural convective Nanofluid flow along with an exponentially accelerating vertical plate in the presence of the magnetic field. They found that velocity profiles are remarkably higher when the magnetic field is fixed

relative to the plate compared to the fluid. Krzysztof *et al.* [19] utilized Convolutional Neural Networks (CNN) to encode the relation between the initial configuration of obstacles and three fundamental quantities in porous media: porosity, permeability, and tortuosity. The fluid flow through a porous medium was simulated with the Lattice Boltzmann method. With the usage of CNN models, they obtained the relation between tortuosity and porosity and then compared it with an empirical estimate. Hamdan *et al.* [20] considered the plane, transverse MHD flow through a porous structure and obtained the solution to the governing equations using an inverse method in which the stream function of the flow is considered. They gained the expressions for the flow quantities for finitely conducting and infinitely conducting fluids.

Vineet Kumar Verma *et al.* [21] investigated the slow flow of liquid past a porous sphere bounded by another porous layer of different permeability and discussed the influence of various parameters such as permeability on streamlines and drag force. The impact of magnetic field on the motion of incompressible micropolar fluid past a sphere has been studied by Krishna Prasad *et al.* [22]. They presented the stream function and micro rotation in terms of the modified Bessel function. In addition, the drag coefficient and tangential velocity for varying physical parameters, including Hartmann number, permeability, micro polarity parameter also represented in the graphical form. In the view of MHD and porous media applications, Thermo-diffusion and diffusion-thermo effects for a Forchheimer model with MHD over a vertical heated plate were studied by Nalinakshi *et al.* [23]. Shilpa *et al.* [24] examined the analytical approach for mixed convective flow in the presence of Casson fluid in a porous channel. The analysis of performance characteristics of neem blended biodiesel run diesel engine was studied Experimentally as well as mathematically by Rajeesh *et al.* [25]. A characteristic study of Coriolis force on free convection in a finite geometry with isotropic and anisotropic porous media has been analyzed by Sudhir *et al.* [26].

Satya Deo *et al.* [27] examined micropolar fluid flow through a porous cylinder embedded in another infinite porous medium and gained the expressions for stream function, micro rotations, couple stresses, fluid pressure, stress tensors, and the same has been discussed graphically. The study of two-dimensional, steady, incompressible viscous fluid flow in composite cylindrical regions was analyzed by Umadevi *et al.* [28]. The nature of the streamlines was observed graphically, and the tangential velocity profile for the various values of porous parameter ' σ '. For various applications ranging from artery modeling to very sensitive tissue modeling such as brain, porous media modeling accurately predicts biological behavior. Nalinakshi *et al.* [29] made an attempt to analyze the MHD mixed convection over a vertical heated plate with a couple of stress fluids numerically and observed the effective convection with significant fluid flow parameters with the inclusion variable fluid properties. Girinath *et al.* [30] attempted to study Numerically the thermal-diffusion and diffusion thermo effects on mixed convective flow and mass transfer in the presence of MHD over an accelerating surface. Erfan *et al.* [31] concentrated on two remarkable biological applications, including (1) blood flow interactions with the porous tissue and (2) hydrodynamic impacts of particle-particle interactions in the microscale modeling that requires a Lagrangian frame. Shilpa *et al.* [32] studied the effect of ohmic and viscous dissipation on Casson fluid's free and forced convective flow in a channel.

In the available literature, less attention has been given to studying fluid flow in the composite spherical region with and without external constraints. Thereby in this work, the flow of fluid through three spherical regions has been considered. This work aims to analyze the flow behavior when the fluid flows over a stationary solid spherical shell of radius ' a ' fixed

in a clear fluid region of radius 'b', which is surrounded by a porous sphere of radius 'c'. The variation of fluid flow in the composite region using streamlines is presented graphically for few representative values of the dimensionless parameters.

2. Formulation of the model and Methods

2.1. Mathematical formulation.

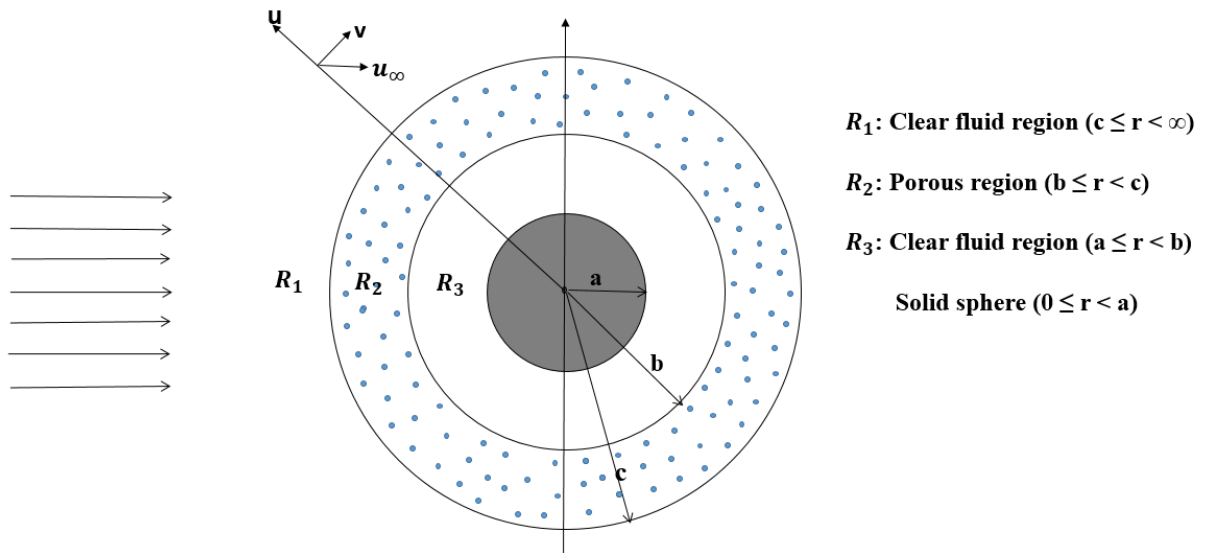


Figure 1. Physical Configuration.

Here 2-D steady, incompressible, viscous fluid flow past a stationary solid spherical core has been considered. The solid sphere of radius 'a' is embedded in a clear fluid region of radius 'b' ($a < b$), surrounded by a porous sphere of radius 'c' ($b < c$) which is placed in the fluid region. Therefore, the flow of fluid takes place in three regions, namely fluid, porous and fluid regions. Further, the flow is considered to be axisymmetric.

For the considered model, the constitutive equations which govern the fluid flow in the fluid region (region R_1), for $c \leq r < \infty$ can be written as:

Equation of continuity,

$$\nabla \cdot \vec{q}_1 = 0, \tag{1}$$

and Stokes equation,

$$\nabla p_1 = \mu \nabla^2 \vec{q}_1, \tag{2}$$

where $\vec{q}_1 = (u_1, v_1, w_1)$ the velocity of the fluid in region R_1 , μ = viscosity of the fluid, p_1 = hydrostatic pressure.

In porous region (region R_2) $b < r \leq c$ the flow of fluid is directed by modified Brinkman equation and equation of continuity which are expressed as,

$$\nabla \cdot \vec{q}_2 = 0, \tag{3}$$

$$\nabla p_2 = \bar{\mu} \nabla^2 \vec{q}_2 - \frac{\mu}{k} \vec{q}_2, \tag{4}$$

where $\vec{q}_2 = (u_2, v_2, w_2)$ is the velocity of the fluid in region R_2 , $\bar{\mu}$ = Brinkman viscosity, p_2 the hydrostatic pressure of the permeable section, and k is the penetrability of the permeable area.

Further, the fluid flow in the fluid section (region R_3) $a < r \leq b$ is represented through Stokes equation and equation of continuity as,

$$\nabla \cdot \vec{q}_3 = 0, \tag{5}$$

$$\nabla p_3 = \bar{\mu} \nabla^2 \vec{q}_3, \tag{6}$$

where $\vec{q}_3 = (u_3, v_3, w_3)$ velocity in region R_3 , $\bar{\mu}$ = Brinkman viscosity, p_3 the hydrostatic pressure.

In this study, it is assumed that Brinkman's viscosity $\bar{\mu}$ is equal to the viscosity of the fluid μ .

A spherical coordinate system (r, θ, ϕ) at the center of the sphere is used and $\theta = 0$ is chosen along the direction of the uniform velocity u_∞ far away from the fluid region. We take $\frac{\partial}{\partial \phi} = 0$ since the flow is axisymmetric. The equations from (1) to (6) are non-dimensionalized

to obtain the dimensionless equations using the following parameters:

$$r^* = \frac{r}{a}, \quad \vec{q}_1^* = \frac{\vec{q}_1}{u_\infty}, \quad \vec{q}_2^* = \frac{\vec{q}_2}{u_\infty}, \quad \vec{q}_3^* = \frac{\vec{q}_3}{u_\infty}, \quad p_1^* = \frac{ap_1}{\mu u_\infty}, \quad p_2^* = \frac{ap_2}{\mu u_\infty}, \quad p_3^* = \frac{ap_3}{\mu u_\infty}. \tag{7}$$

Therefore, the governing Eq. (1) and Eq. (2), for spherical polar coordinate system becomes,

$$\frac{\partial}{\partial r}(r^2 u_1) + \frac{r}{\sin \theta} \frac{\partial}{\partial \theta}(v_1 \sin \theta) = 0, \tag{8}$$

$$-\frac{\partial p_1}{\partial r} = -\left[\frac{\partial^2 u_1}{\partial r^2} + \frac{2}{r} \frac{\partial u_1}{\partial r} + \frac{1}{r^2} \frac{\partial^2 u_1}{\partial \theta^2} + \frac{\cot \theta}{r^2} \frac{\partial u_1}{\partial \theta} - \frac{2u_1}{r^2} - \frac{2}{r^2} \frac{\partial v_1}{\partial \theta} - \frac{2v_1 \cot \theta}{r^2} \right], \tag{9}$$

$$-\frac{1}{r} \frac{\partial p_1}{\partial \theta} = -\left[\frac{\partial^2 v_1}{\partial r^2} + \frac{2}{r} \frac{\partial v_1}{\partial r} + \frac{1}{r^2} \frac{\partial^2 v_1}{\partial \theta^2} + \frac{\cot \theta}{r^2} \frac{\partial v_1}{\partial \theta} + \frac{2}{r^2} \frac{\partial u_1}{\partial \theta} - \frac{v_1 \cos \theta}{r^2} \right] \tag{10}$$

Similarly, using the non-dimensional parameters from eq. (7), the Eq. (3) and Eq. (4) are non-dimensionalized for the permeable region, and the corresponding equations in the spherical polar coordinate system are:

$$\frac{\partial}{\partial r}(r^2 u_2) + \frac{r}{\sin \theta} \frac{\partial}{\partial \theta}(v_2 \sin \theta) = 0, \tag{11}$$

$$-\frac{\partial p_2}{\partial r} = \sigma^2 u_2 - \left[\frac{\partial^2 u_2}{\partial r^2} + \frac{2}{r} \frac{\partial u_2}{\partial r} + \frac{1}{r^2} \frac{\partial^2 u_2}{\partial \theta^2} + \frac{\cot \theta}{r^2} \frac{\partial u_2}{\partial \theta} - \frac{2u_2}{r^2} - \frac{2}{r^2} \frac{\partial v_2}{\partial \theta} - \frac{2v_2 \cot \theta}{r^2} \right], \tag{12}$$

$$-\frac{1}{r} \frac{\partial p_2}{\partial \theta} = \sigma^2 v_2 - \left[\frac{\partial^2 v_2}{\partial r^2} + \frac{2}{r} \frac{\partial v_2}{\partial r} + \frac{1}{r^2} \frac{\partial^2 v_2}{\partial \theta^2} + \frac{\cot \theta}{r^2} \frac{\partial v_2}{\partial \theta} + \frac{2}{r^2} \frac{\partial u_2}{\partial \theta} - \frac{v_2 \cos \theta}{r^2} \right], \tag{13}$$

where $\sigma = \frac{a}{\sqrt{k}}$ is the porous parameter in which k is the perviousness of the fluid.

Similarly, using the transformation from Eq. (7), the Eq. (5) and Eq. (6) are non-dimensionalized for the fluid region, and the corresponding equations in the spherical polar coordinate system turn into,

$$\frac{\partial}{\partial r}(r^2 u_3) + \frac{r}{\sin \theta} \frac{\partial}{\partial \theta}(v_3 \sin \theta) = 0, \tag{14}$$

$$-\frac{\partial p_3}{\partial r} = -\left[\frac{\partial^2 u_3}{\partial r^2} + \frac{2}{r} \frac{\partial u_3}{\partial r} + \frac{1}{r^2} \frac{\partial^2 u_3}{\partial \theta^2} + \frac{\cot \theta}{r^2} \frac{\partial u_3}{\partial \theta} - \frac{2u_3}{r^2} - \frac{2}{r^2} \frac{\partial v_3}{\partial \theta} - \frac{2v_3 \cot \theta}{r^2} \right], \tag{15}$$

$$-\frac{1}{r} \frac{\partial p_3}{\partial \theta} = -\left[\frac{\partial^2 v_3}{\partial r^2} + \frac{2}{r} \frac{\partial v_3}{\partial r} + \frac{1}{r^2} \frac{\partial^2 v_3}{\partial \theta^2} + \frac{\cot \theta}{r^2} \frac{\partial v_3}{\partial \theta} + \frac{2}{r^2} \frac{\partial u_3}{\partial \theta} - \frac{v_3 \cos ec^2 \theta}{r^2} \right]. \tag{16}$$

Since the flow is axisymmetric, the stream function $\psi_i(r, \theta)$ (where $i = 1, 2, 3$ corresponds to fluid, porous and fluid regions, respectively) satisfies the equation of continuity for both fluid and porous regions in the spherical polar coordinate system is considered. It is defined as follows:

$$u_i = \frac{1}{r^2 \sin \theta} \frac{\partial \psi_i}{\partial \theta}; \quad v_i = \frac{-1}{r \sin \theta} \frac{\partial \psi_i}{\partial r}. \tag{17}$$

By cross differentiation, we removed the pressure term from Eq. (9), and Eq. (10) of the fluid region, Eq. (12), and Eq. (13) of the porous region and Eq. (15), and Eq. (16) of the fluid region, to obtain the linear partial differential equation of fourth order in terms of stream function. It can be represented as follows:

$$E^4 \psi_1 = 0, \quad c \leq r < \infty, \tag{18}$$

$$E^4 \psi_2 - \sigma^2 E^2 \psi_2 = 0, \quad b \leq r < c, \tag{19}$$

$$E^4 \psi_3 = 0, \quad a \leq r < b. \tag{20}$$

An Eq. (18), (19), and (20) are the fourth-order Partial Differential Equations (PDE), where $E^2 = \frac{\partial^2}{\partial r^2} + \frac{\sin \theta}{r^2} \frac{\partial}{\partial \theta} \left(\frac{1}{\sin \theta} \frac{\partial}{\partial \theta} \right)$ is the Laplacian operator in a spherical coordinate system.

The variation of fluid flow at the boundary is defined using different interfacial boundary conditions for the multiple regions are as follows : (i) the no-slip condition on the surface of the solid sphere; (ii) the continuation in normal and tangential stress components at the boundary of the porous and fluid regions; and (iii) the velocity far away from the clear fluid region.

The no-slip condition at the surface of the solid sphere is:

$$u_3(a, \theta) = 0, \quad 0 \leq \theta \leq 2\pi, \tag{21}$$

$$v_3(a, \theta) = 0, \quad 0 \leq \theta \leq 2\pi. \tag{22}$$

Interfacial conditions, a continuation of normal and tangential velocity components, and the corresponding stress components at the interface of the porous and fluid regions are as follows:

Interfacial boundary conditions across the region R_1 and region R_2 are,

$$u_2(c, \theta) = u_1(c, \theta), \quad 0 \leq \theta \leq 2\pi, \tag{23}$$

$$v_2(c, \theta) = v_1(c, \theta), \quad 0 \leq \theta \leq 2\pi, \tag{24}$$

$$\tau_{r\theta(2)}(c, \theta) = \tau_{r\theta(1)}(c, \theta), \quad 0 \leq \theta \leq 2\pi, \tag{25}$$

$$\tau_{rr(2)}(c, \theta) = \tau_{rr(1)}(c, \theta), \quad 0 \leq \theta \leq 2\pi. \tag{26}$$

Interfacial boundary conditions across the region R_2 and region R_3 are,

$$u_3(b, \theta) = u_2(b, \theta), \quad 0 \leq \theta \leq 2\pi, \tag{27}$$

$$v_3(b, \theta) = v_2(b, \theta), \quad 0 \leq \theta \leq 2\pi, \tag{28}$$

$$\tau_{r\theta(3)}(b, \theta) = \tau_{r\theta(2)}(b, \theta), \quad 0 \leq \theta \leq 2\pi, \tag{29}$$

$$\tau_{rr(3)}(b, \theta) = \tau_{rr(2)}(b, \theta), \quad 0 \leq \theta \leq 2\pi, \tag{30}$$

where $\tau_{r\theta(1)}$ and $\tau_{rr(1)}$ represents the dimensionless tangential and normal components of stress tensors in the fluid region and is given by

$$\tau_{r\theta(1)} = \frac{1}{r} \frac{\partial u_1}{\partial \theta} + \frac{\partial v_1}{\partial r} - \frac{v_1}{r}, \tag{31}$$

$$\tau_{rr(1)} = -p_1 + 2 \frac{\partial u_1}{\partial r}. \tag{32}$$

Further, $\tau_{r\theta(2)}$, $\tau_{rr(2)}$ and $\tau_{r\theta(3)}$, $\tau_{rr(3)}$ stands for dimensionless tangential and normal components stress tensors in the porous region, fluid region, respectively. These are also defined in the same way as Eq. (31) and Eq. (32).

As it was assumed earlier that, fluid viscosity is equal to the Brinkman viscosity, the Eq. (26) and Eq. (30), which indicates the constant pressure at the interface. Thus, Eq. (26) and Eq. (30) reduces to:

$$p_2(c, \theta) = p_1(c, \theta), \quad 0 \leq \theta \leq 2\pi \tag{33}$$

$$p_3(b, \theta) = p_2(b, \theta), \quad 0 \leq \theta \leq 2\pi. \tag{34}$$

Further, the stream function in the fluid region far from the boundary is given by:

$$\psi_1(r, \theta) = \frac{1}{2} \left(r^2 - \frac{1}{r} \right) \sin^2 \theta, \quad c \leq r < \infty. \tag{35}$$

From Eq. (17) and Eq. (35), the boundary conditions for the velocity components far from the fluid region are:

$$u_1 \sim \cos \theta, \quad v_1 \sim -\sin \theta \quad \text{as } r \rightarrow \infty. \tag{36}$$

Hence the boundary condition far-off from the fluid region, Eq. (35) reduces in terms of stream function as:

$$\psi_1(r, \theta) \sim \frac{r^2}{2} \sin^2 \theta, \text{ as } r \rightarrow \infty. \tag{37}$$

2.2. Methodology.

The boundary conditions from Eq. (37) suggests the following similarity solution to Eq. (18), (19), and (20) as:

$$\psi_1(r, \theta) = f_1(r) \sin^2 \theta, \quad c \leq r < \infty, \tag{38}$$

$$\psi_2(r, \theta) = f_2(r) \sin^2 \theta, \quad b \leq r < c, \tag{39}$$

$$\psi_3(r, \theta) = f_3(r) \sin^2 \theta, \quad a \leq r < b. \tag{40}$$

Substituting Eq. (38) in (18), Eq. (39) in (19), and Eq. (40) in (20), the 4th order partial differential equations having stream functions $\psi_1(r, \theta)$, $\psi_2(r, \theta)$ and $\psi_3(r, \theta)$ reduces to the fourth-order ordinary differential equation in $f_1(r)$, $f_2(r)$ and $f_3(r)$ respectively, and are given by:

$$f_1^{iv}(r) - \frac{4}{r^2} f_1''(r) + \frac{8}{r^3} f_1'(r) - \frac{8}{r^4} f_1(r) = 0, \quad c \leq r < \infty, \tag{41}$$

$$f_2^{iv}(r) - \frac{4}{r^2} f_2''(r) + \frac{8}{r^3} f_2'(r) - \frac{8}{r^4} f_2(r) - \sigma^2 \left(f_2''(r) - \frac{2}{r^2} f_2(r) \right) = 0, \quad b \leq r < c \tag{42}$$

$$f_3^{iv}(r) - \frac{4}{r^2} f_3''(r) + \frac{8}{r^3} f_3'(r) - \frac{8}{r^4} f_3(r) = 0, \quad a \leq r < b. \tag{43}$$

The corresponding boundary conditions in terms of $f_1(r)$, $f_2(r)$ and $f_3(r)$ from Eq. (21) to (30) and from Eq. (37) are as follows:

The No-slip condition at the surface of the solid sphere is expressed by:

$$f_3(a) = 0, \tag{44}$$

$$f_3'(a) = 0, \tag{45}$$

and matching boundary condition at the interface of the porous and fluid region takes the form: Across the region R_1 and region R_2 , the interfacial conditions are,

$$f_2(c) = f_1(c), \tag{46}$$

$$f_2'(c) = f_1'(c), \tag{47}$$

$$f_2''(c) = f_1''(c), \tag{48}$$

$$f_2'''(c) - \sigma_1^2 f_2'(c) = f_1'''(c). \tag{49}$$

Across the region R_2 and region R_3 , the interfacial conditions are,

$$f_3(b) = f_2(b), \tag{50}$$

$$f_3'(b) = f_2'(b), \tag{51}$$

$$f_3''(b) = f_2''(b), \tag{52}$$

$$f_3'''(b) - \sigma_2^2 f_3'(b) = f_2'''(b). \tag{53}$$

The constant velocity far from the boundary, from Eq. (37) reduces to,

$$f_1(r) \sim \frac{r^2}{2} \text{ as } r \rightarrow \infty. \tag{54}$$

The solution for the Eq. (41) and Eq. (43) corresponding to fluid regions (region R_1 and region R_3) respectively is given by,

$$f_1(r) = \frac{A_1}{r} + B_1 r^2 + C_1 r + D_1 r^4, \quad c \leq r < \infty, \tag{55}$$

$$f_3(r) = \frac{A_3}{r} + B_3 r^2 + C_3 r + D_3 r^4, \quad a \leq r < b. \tag{56}$$

The solution for Eq. (42) corresponding to the porous region (region R₂) is obtained analytically by taking the substitution,

$$g(r) = f_i''(r) - \frac{2}{r^2} f_i(r) \quad , \quad (57)$$

where the suffix *i* takes the value 2 to represent the method of solution in the porous region.

Substitution of Eq. (57) in Eq. (42) reduces to second-order ordinary differential equation in *g(r)* as,

$$g''(r) - \left(\sigma^2 + \frac{2}{r^2} \right) g(r) = 0. \quad (58)$$

Further, consider the transformation function for *g(r)* as,

$$g(r) = \sqrt{r} w(r), \quad (59)$$

where *w(r)* the arbitrary function.

Thereby, Eq. (58) reduces to:

$$r^2 w''(r) + r w'(r) - \left[\left(\frac{3}{2} \right)^2 + \sigma^2 r^2 \right] w(r) = 0, \quad (60)$$

which represents the modified Bessel's differential equation of order 3/2, bearing the solution in terms of modified Bessel's function is given as,

$$w(r) = C_2 I_{3/2}(\sigma r) + D_2 K_{3/2}(\sigma r), \quad (61)$$

where *C*₂ and *D*₂ are arbitrary constants.

Thus from Eq. (59), we have:

$$g(r) = C_2 \sqrt{r} I_{3/2}(\sigma r) + D_2 \sqrt{r} K_{3/2}(\sigma r). \quad (62)$$

Therefore, the Eq. (57) reduces to,

$$f_2''(r) - \frac{2}{r^2} f_2(r) = C_2 \sqrt{r} I_{3/2}(\sigma r) + D_2 \sqrt{r} K_{3/2}(\sigma r) \quad (63)$$

Eq. (63) is a second-order ordinary differential equation with a variable coefficient. Using the method of variation of parameters, the obtained general solution is given by,

$$f_2(r) = \frac{A_2}{r} + B_2 r^2 + C_2 \sqrt{\sigma r} I_{3/2}(\sigma r) + D_2 \sqrt{\sigma r} K_{3/2}(\sigma r). \quad (64)$$

For the flow in fluid region as $r \rightarrow \infty$ the solution for fluid region Eq. (55) is valid if and only if *D*₁ = 0. Also, from Eq. (54) we get $B_1 = \frac{1}{2}$. Henceforth Eq. (55) reduces to:

$$f_1(r) = \frac{A_1}{r} + \frac{r^2}{2} + C_1 r \quad , \quad c \leq r < \infty. \quad (65)$$

Also, Eq. (64) for $b \leq r < c$ can be written as:

$$f_2(r) = \frac{A_2}{r} + B_2 r^2 + C_2 \left(\frac{\cosh(\sigma r)}{\sigma r} - \sinh(\sigma r) \right) + D_2 \left(\frac{\sinh(\sigma r)}{\sigma r} - \cosh(\sigma r) \right), \quad (66)$$

and, the Eq. (56) for $a \leq r < b$ can be written as:

$$f_3(r) = \frac{A_3}{r} + B_3 r^2 + C_3 r + D_3 r^4. \quad (67)$$

Henceforth the stream function corresponding to fluid, permeable and fluid regions are agreed by,

$$\psi_1(r, \theta) = \left(\frac{A_1}{r} + \frac{r^2}{2} + C_1 r \right) \sin^2 \theta, \quad c \leq r < \infty, \tag{68}$$

$$\psi_2(r, \theta) = \left(\frac{A_2}{r} + B_2 r^2 + C_2 \left(\frac{\cosh(\sigma r)}{\sigma} - \sinh(\sigma r) \right) + D_2 \left(\frac{\sinh(\sigma r)}{\sigma} - \cosh(\sigma r) \right) \right) \sin^2 \theta, \quad b \leq r < c, \tag{69}$$

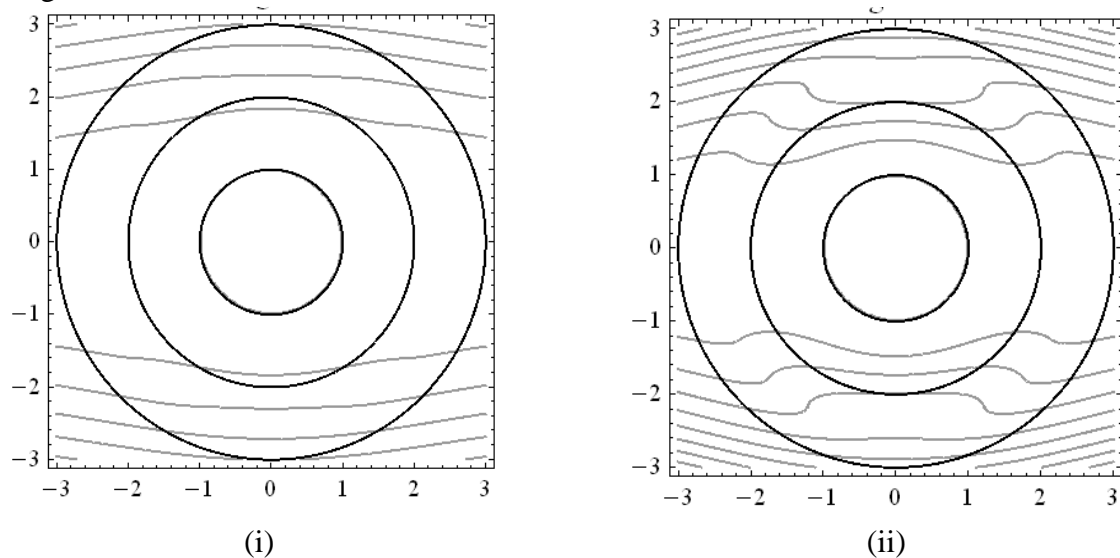
$$\psi_3(r, \theta) = \left(\frac{A_3}{r} + B_3 r^2 + C_3 r + D_3 r^4 \right) \sin^2 \theta, \quad a \leq r < b. \tag{70}$$

Here the arbitrary constants $A_1, C_1, A_2, B_2, C_2, D_2, A_3, B_3, C_3,$ and D_3 are determined using the above boundary conditions from Eq. (44) to (53).

3. Results and Discussions

The flow of viscous, steady, two-dimensional, incompressible fluid past a fixed solid sphere of radius ‘a’ surrounded by a clear fluid region of radius ‘b’ ($a < b$); enclosed by the porous sphere of radius ‘c’ ($b < c$) which is placed in the fluid region has been investigated analytically. To analyze the flow behavior in fluid and porous regions, the Stokes and Brinkman equations, respectively, are used. Further, it is assumed that the flow is axisymmetric. The similarity solution method is used to find the exact solution analytically. In this method, the partial differential equations of the physical configuration are transformed into ordinary differential equations. These ordinary differential equations are converted into modified Bessel’s equations using a special transformation. The solution obtained is in terms of the modified Bessel function of order 3/2. The continuation of velocity and stress components at the interface of fluid and porous regions and no-slip conditions at the surface of the solid sphere are considered. The expression for the stream functions corresponding to fluid, porous, and fluid regions is obtained in terms of ‘r’ and dimensionless parameters.

The effect of porous parameter σ on the flow behavior in the three regions is presented through the streamlines.



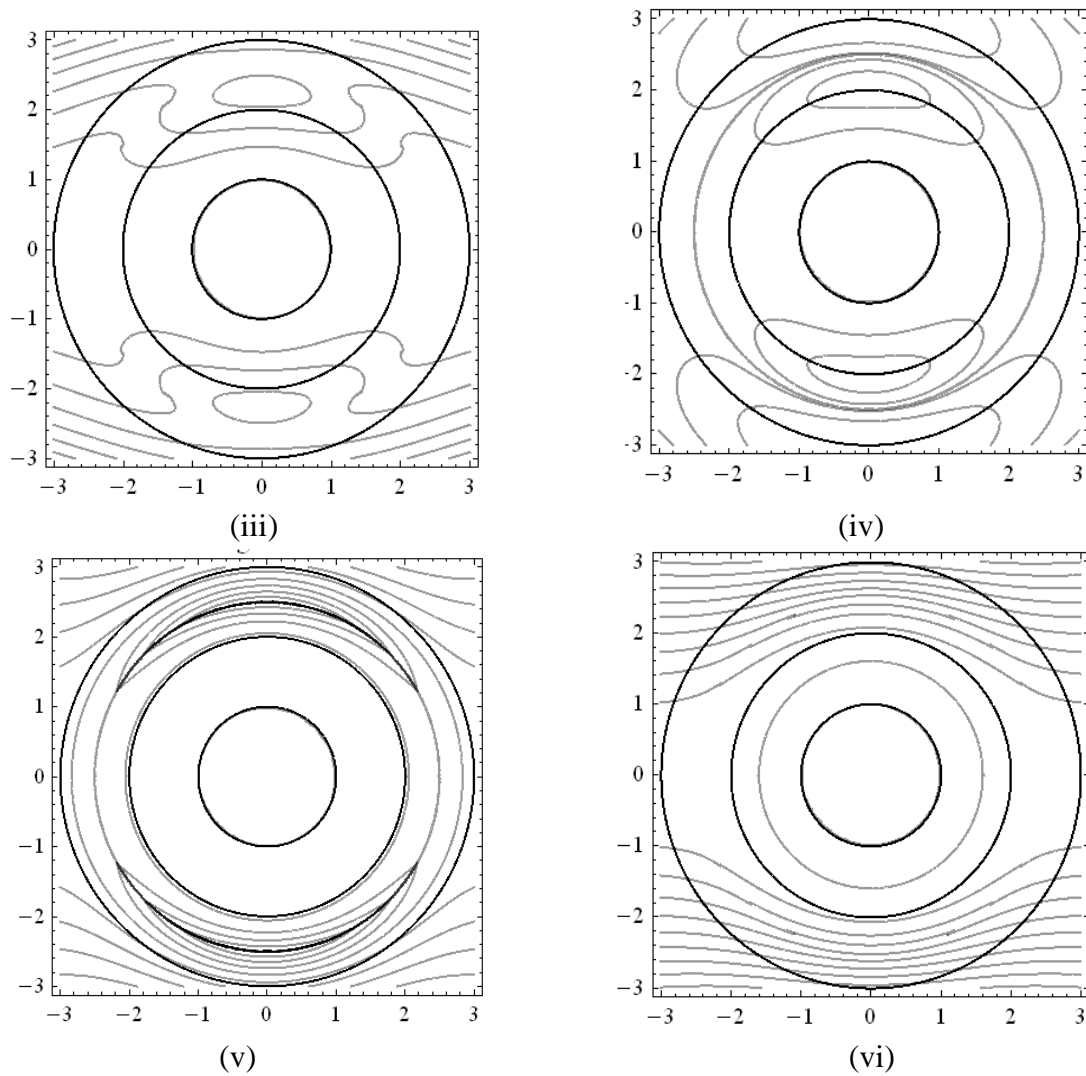


Figure 2. Streamlines for different values of porous parameter σ .

(i) $\sigma = 4$ (ii) $\sigma = 4.5$ (iii) $\sigma = 4.6$ (iv) $\sigma = 4.7$ (v) $\sigma = 4.94$ (vi) $\sigma = 5$

Initially, for $\sigma = 4$, the free flow of fluid in the porous region is observed, and the same is witnessed in Figure 2(i). Increasing the porous parameter to $\sigma = 4.5$, the fluid flow in the porous region slows down for a while due to a slight decrease in the permeability. It then enters into the fluid region (region 3). As a result, the streamlines can be seen near the solid surface. (see Figure 2(ii)). Further increasing the porous parameter to $\sigma = 4.6$ and 4.7 , the circulatory motion of the fluid is observed in the porous region. The reason for such behavior is that as the porous parameter increases, the fluid resists flowing into the porous region due to decreased permeability. Thus the amount of fluid flow in the fluid region (region 3) is reduced. Hence, the streamlines are moving away from the solid sphere shown in Figures 2(iii) and 2(iv). Furthermore, the porous parameter increased to $\sigma = 4.94$ and then to $\sigma = 5$, there is a suppression of fluid flow in the porous region, and hence the meandering of streamlines can be seen past a solid sphere. (see Figures 2(v) and 2(vi)).

The tangential and normal velocity of the fluid at the boundary of the clear fluid region (region R_1), porous region (region R_2), and clear fluid region (region R_3) for different values of the porous parameter are analyzed graphically.

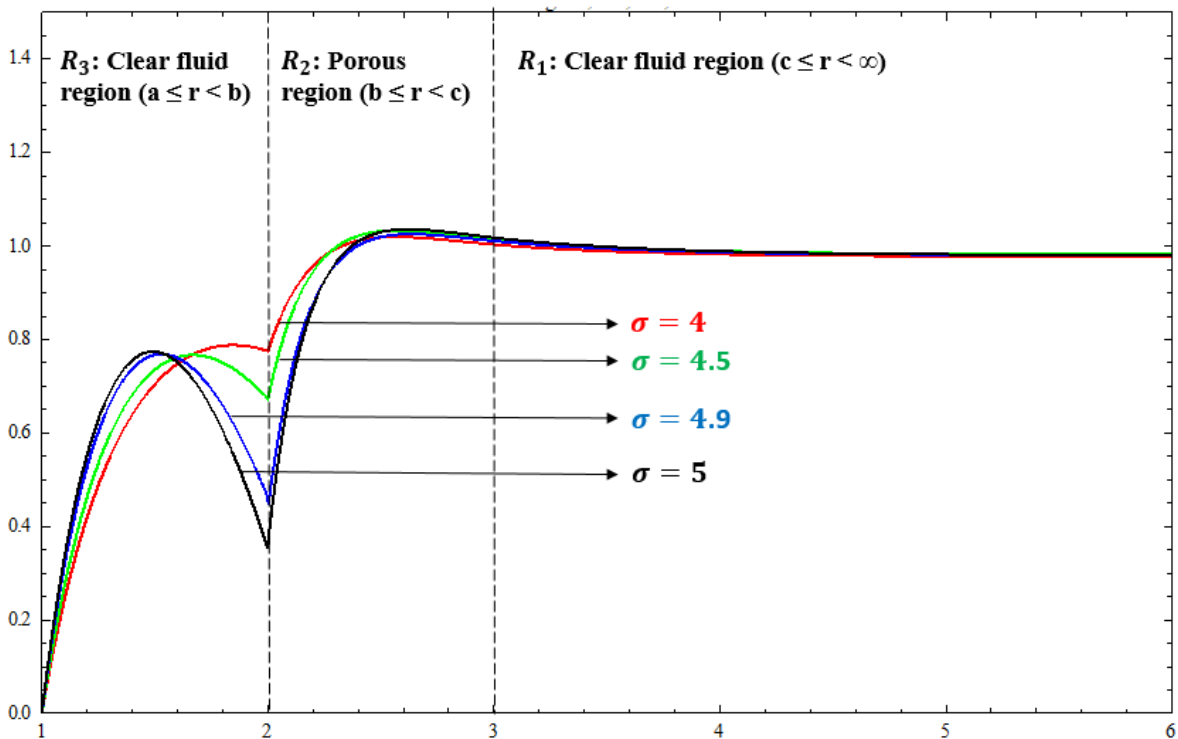


Figure 3. Tangential velocity for different values of the porous parameter.

- (i) $\sigma = 4$ (ii) $\sigma = 4.5$ (iii) $\sigma = 4.9$ (iv) $\sigma = 5$.

To our knowledge in the literature, this is the first of its kind to find the entire velocity profile for multiple regions. Here, we made an attempt to study the tangential and normal velocity characteristics for the physical configuration of the problem for the variation of porous parameter σ in Figures 3 and 4, respectively. In the physical configuration, we observe that R_1 is the region bounded by porous media at one end and free boundary on the other end; R_2 is a finite boundary between R_1 and R_3 with radius ‘b’ and ‘c’, whereas R_3 is a region bounded between solid core and porous media with radius ‘a’ and ‘b’. A uniform flow of fluid velocity U_∞ is approaching towards the region of interest from the faraway region ($R \rightarrow \infty$). Due to the resisting force offered by the porous media in the outer region of R_2 the velocity diminishes gradually from the uniform speed, the velocity of the flow will increase near the boundary of R_2 and a matching condition is seen between R_2 and R_1 . This result exactly matches with physical phenomena as well as the exact analytical solution of the problem. The thickness of the region R_2 of the porous medium will decrease the velocity of fluid flow and enter the boundary of the region R_3 of clear fluid nature. This region acts as a Poiseuille flow between a porous medium and solid core region. Here, the characteristic of the velocity profile will take in the form of a parabola which is maximum at the middle portion and least at the boundary of the regions. One side of the parabola satisfies the matching condition of the porous medium and another at the solid core region with no-slip condition. The same is replicated in the above Figure 3 of the tangential velocity profile. The analysis of the tangential velocity component is observed for the variation of the porous parameter σ ; it is seen that the effect of the porous parameter will diminish the velocity flow of the fluid due to an increase in the permeability of the porous medium. A similar analysis is carried out to study the normal component of velocity in three regions of the physical phenomena of the geometry. Here also equivalent observation is seen in the characteristic of the profile in Figure 4. In the literature, this is the first of its kind to observe completely for the entire domain of the multiple regions of the sphere.

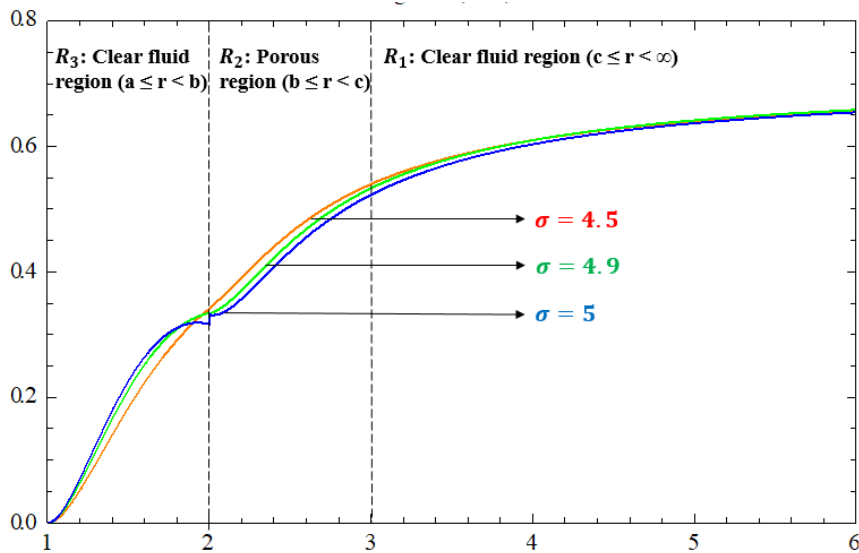


Figure 4. Normal velocity for different values of the porous parameter.

- (i) $\sigma = 4.5$ (ii) $\sigma = 4.9$ (iii) $\sigma = 5$

The same phenomena can be observed in real-time applications like oil extraction from the earth crust, drug permeation through human skin, etc. Based on the above results, it is observed that the considered porous parameter plays a very important role in controlling the fluid flow, which can be seen in the mathematical formulation and the practical applications cited in the above literature work. Further, these results will help us improve or control the fluid flow in the applications such as water filtration (Reverse Osmosis Process), extraction of energy from the geothermal region, and so on. This investigation effectively uses two-dimensional, steady, viscous, incompressible, and electrically conducting fluid past a solid sphere with additional external constraints. The results of this study may be of interest to researchers for extending this work to find the drag coefficient in the case of composite spherical and cylindrical regions with and without constraints.

4. Conclusions

The concept of fluid flow through porous media has its importance in many fields of applied science and engineering, such as filtration, acoustics, geology, soil mechanics, rock mechanics, petroleum engineering, bioremediation, construction engineering, and in the field of geology like biology, petroleum geology, geophysics, biology, also in interdisciplinary areas of materials science. In addition, the principle of porous flow has applications of inkjet printing and nuclear waste disposal techniques, among others. With reference to the above-said applications, this work presents the analytical solution for 2-D, steady, incompressible, viscous fluid flow over the static solid sphere of radius ‘a’ placed in a spherical porous medium. The hydrostatic behavior of fluid flow has been studied by varying the porous parameter through streamlines. The graph shows that the streamlines have meandered in the porous region for the increase in porous parameter, but further increase in porous parameter suppresses the fluid flow in the porous region. As a result, the fluid moves away from the solid sphere. It is also observed that as the porous parameter increases, the velocity of the fluid decreases at the boundary of the porous sphere due to less permeability. As a result, fluid experiences a force and rushes into the clear fluid region with an increase in velocity due to the pressure at the boundary of

the porous sphere. Hence the parabolic velocity profile is noticed at the center of the clear fluid region (region R_3).

Funding

This research received no external funding.

Acknowledgments

The authors are grateful to research Center Atria Institute of Technology, Vivekananda Institute of Technology, M S Ramaiah Institute of Technology, Vemana Institute of Technology, B M S College of Engineering, Bangalore, India, for their support and encouragement to carry out our research work.

Conflicts of Interest

The authors declare no conflict of interest.

References

1. Ooms, G.; Mijnlieff, P.F.; Beckers, H.L. Frictional Force Exerted by a Flowing Fluid on a Permeable Particle, with Particular Reference to Polymer Coils. *The Journal of Chemical Physics* **1970**, *53*, 4123-4130, <https://doi.org/10.1063/1.1673911>.
2. Saffman, P.G. On the Boundary Condition at the Surface of a Porous Medium. *Studies in Applied Mathematics* **1971**, *50*, 93-101, <https://doi.org/10.1002/sapm197150293>.
3. Neale, G.; Epstein, N.; Nader, W. Creeping flow relative to permeable spheres. *Chemical Engineering Science* **1973**, *28*, 1865-1874, [https://doi.org/10.1016/0009-2509\(73\)85070-5](https://doi.org/10.1016/0009-2509(73)85070-5).
4. Howells, I.D. Drag due to the motion of a Newtonian fluid through a sparse random array of small fixed rigid objects. *Journal of Fluid Mechanics* **1974**, *64*, 449-476, <https://doi.org/10.1017/S0022112074002503>.
5. Masliyah, J.H.; Neale, G.; Malysa, K.; G.M. Van De Ven, T. Creeping flow over a composite sphere: Solid core with porous shell. *Chemical Engineering Science* **1987**, *42*, 245-253, [https://doi.org/10.1016/0009-2509\(87\)85054-6](https://doi.org/10.1016/0009-2509(87)85054-6).
6. Yu, Q.; Kaloni, P.N. A cartesian-tensor solution of the Brinkman equation. *Journal of Engineering Mathematics* **1988**, *22*, 177-188, <https://doi.org/10.1007/BF02383599>.
7. Pop, I.; Ingham, D.B. Flow past a sphere embedded in a porous medium based on the Brinkman model. *International Communications in Heat and Mass Transfer* **1996**, *23*, 865-874, [https://doi.org/10.1016/0735-1933\(96\)00069-3](https://doi.org/10.1016/0735-1933(96)00069-3).
8. Bhattacharyya, A.; Raja Sekhar, G.P. Viscous flow past a porous sphere with an impermeable core : effect of stress jump condition. *Chemical Engineering Science* **2004**, *59*, 4481-4492, <https://doi.org/10.1016/j.ces.2004.06.017>.
9. Magyari, E. Comment on "Flow of a Weakly Conducting Fluid in a Channel Filled with a Porous Medium" by A. Pantokratoras and T. Fang. *Transport in Porous Media* **2010**, *83*, 677-680, <https://doi.org/10.1007/s11242-009-9486-y>.
10. Reddy, N.B.P.; Krishnaiyah, S.; Reddy, M.R. Effect Of Angle Of Inclination On Non-Uniform Flow Through Porous Media. **2015**, *18*, 879-892, <https://doi.org/10.1615/JPorMedia.v18.i9.50>.
11. Jayalakshamma, D.V.; Dinesh, P.A.; Chandrashekar, D.V. Numerical Study of Micropolar Fluid Flow Past an Impervious Sphere. *Defect and Diffusion Forum* **2018**, *388*, 344-349, <https://doi.org/10.4028/www.scientific.net/DDF.388.344>.
12. Mahabaleshwar, U.S.; Vinay Kumar, P.N.; Nagaraju, K.R.; Bognár, G.; Nayakar, S.N.R. A New Exact Solution for the Flow of a Fluid through Porous Media for a Variety of Boundary Conditions. *Fluids* **2019**, *4*, <https://doi.org/10.3390/fluids4030125>.
13. Siva Murali, M. R.; Venkatesh Kulkarni, M.. Numerical investigation on fluid flow through porous media and empirical correlation for pressure drop. *International Journal of Recent Technology and Engineering* **2019**, *8*, Issue-1C. <http://dx.doi.org/10.2139/ssrn.3506573>.
14. Deo, S.; Ansari, I.A. Brinkman Flow Through A Porous Cylinder Embedded In Another Unbounded Porous Medium. **2019**, *22*, 681-692, <https://doi.org/10.1615/JPorMedia.2019029027>.
15. Ramalakshmi, K.; Shukla, P. Drag On A Fluid Sphere Embedded In A Porous Medium With Solid Core, **2019**, *46*, 219-228, <https://doi.org/10.1615/InterJFluidMechRes.2018025197>.

16. Khanukaeva, D.Y.; Filippov, A.N.; Yadav, P.K.; Tiwari, A. Creeping flow of micropolar fluid parallel to the axis of cylindrical cells with porous layer. *European Journal of Mechanics - B/Fluids* **2019**, *76*, 73-80, <https://doi.org/10.1016/j.euromechflu.2019.01.012>.
17. Umadevi, B.; Dinesh, P.A.; Vinay, C.V. The Analytical Study of Velocity Slip on Two-Phase Flow in an Eccentric Annular Region. In Proceedings of the Advances in Applied Mechanical Engineering, Singapore, **2020**, *2020*, 223-231, https://doi.org/10.1007/978-981-15-1201-8_26.
18. Sravan Kumar, T.; Dinesh, P.A.; Makinde, O.D. Impact of Lorentz Force and Viscous Dissipation on Unsteady Nanofluid Convection Flow over an Exponentially Moving Vertical Plate. *Mathematical Models and Computer Simulations* **2020**, *12*, 631-646, <https://doi.org/10.1134/S2070048220040110>.
19. Graczyk, K.M.; Matyka, M. Predicting porosity, permeability, and tortuosity of porous media from images by deep learning. *Scientific Reports* **2020**, *10*, 21488, <https://doi.org/10.1038/s41598-020-78415-x>.
20. Hamdan, M. , Silva-Zea, R. , Erazo-Bone, R. , Chuchuca-Aguilar, F. and Escobar-Segovia, K. Plane Transverse MHD Flow through Porous Media. *Journal of Applied Mathematics and Physics* **2020**, *8*, 2115-2128, <https://doi.org/10.4236/jamp.2020.810158>.
21. Verma, V.K.; Verma, H. Flow Past Porous Sphere Covered With Another Porous Layer Of Different Permeability. **2020**, *11*, 149-160, <https://doi.org/10.1615/SpecialTopicsRevPorousMedia.2020031001>.
22. Madasu, K.P.; Bucha, T. Influence of MHD on micropolar fluid flow past a sphere implanted in porous media. *Indian Journal of Physics* **2021**, *95*, 1175-1183, <https://doi.org/10.1007/s12648-020-01759-7>.
23. Nalinakshi, N.; Dinesh, P.A. Thermo-Diffusion and Diffusion-Thermo Effects for a Forchheimer Model with MHD Over a Vertical Heated Plate. In Proceedings of the Advances in Fluid Dynamics, Singapore **2021**, *2021*, 343-361.
24. Shilpa, B.V.; Chandrashekar, D.V.; Dinesh, P.A.; Eswara, A.T. Analytical Approach for Mixed Convective Flow in Presence of Casson Fluid in a Porous Channel. In Proceedings of the Advances in Fluid Dynamics, Singapore **2021**, *2021*, 939-951.
25. Rajeesh, S.; Prakash, S.V.; Dinesh, P.A. Experimental and Mathematical Analysis of Performance Characteristics of Neem Blended Biodiesel Run Diesel Engine. In Proceedings of the Advances in Fluid Dynamics, Singapore **2021**, *2021*, 973-983.
26. Patel, S.; Dinesh, P.A.; Suma, S.P.; Ramesh, N.L. Characteristic Study of Coriolis Force on Free Convection in a Finite Geometry with Isotropic and Anisotropic Porous Media. In Proceedings of the Advances in Fluid Dynamics, Singapore **2021**, *2021*, 985-997.
27. Deo, S.; Maurya, P.K. Micropolar Fluid Flow Through A Porous Cylinder Embedded In Another Unbounded Porous Medium. **2021**, *24*, 89-99, <https://doi.org/10.1615/JPorMedia.2021034738>.
28. R. Umadevi.; D. V. Chandrashekar.; P. A. Dinesh.; D. V. Jayalakshamma. Fluid flow in composite cylindrical regions. *Advanced Engineering Forum* **2021**, *40*, 63-72, <https://doi.org/10.4028/www.scientific.net/AEF.40>.
29. Nalinakshi, N.; Dinesh, P. A.; Harichandra, B. P.; Likith, G. Effect of Variable Fluid Properties and Magneto Hydrodynamics for Convection with Couple Stress Fluid. *Biointerface Research in Applied Chemistry* **2021**, *11*, 13490 – 13501, <https://doi.org/10.33263/BRIAC115.1349013501>.
30. Girinath Reddy, M.; Dinesh, P. A.; Basavaraj Shankarappa, M.; Uma, M. Numerical Study of Thermal-Diffusion and Diffusion Thermo Effects on Mixed Convective Flow and Mass Transfer in the Presence of MHD over an Accelerating Surface. *Biointerface Research in Applied Chemistry* **2021**, *11*, 11487 – 11498, <https://doi.org/10.33263/BRIAC114.1148711498>.
31. Kosari, E.; Vafai, K. Synthesis of flow and thermal transport in porous media as applied to biological applications. *Journal of Heat Transfer* **2021**, *143*, <https://doi.org/10.1115/1.4050616>.
32. Shilpa, B. V.; Dinesh, P. A.; Jyothirmayi, M.; Chandrashekar, D. V. Ohmic and Viscous Dissipation Effect on Free and Forced Convective Flow of Casson Fluid in a Channel. *Biointerface Research in Applied Chemistry* **2022**, *12*, 132 – 148, <https://doi.org/10.33263/BRIAC121.132148>.